

# Intracellular delay limits cyclic changes in gene expression

Katja Rateitschak\*, Olaf Wolkenhauer

Systems Biology and Bioinformatics Group

University of Rostock

18051 Rostock, Germany

katja.rateitschak@uni-rostock.de

olaf.wolkenhauer@uni-rostock.de

www.sbi.uni-rostock.de

March 31, 2022

## Abstract

Based on previously published experimental observations and mathematical models for Hes1, p53 and NF- $\kappa$ B gene expression, we improve these models through a distributed delay formulation of the time lag between transcription factor binding and mRNA production. This description of natural variability for delays introduces a transition from a stable steady state to limit cycle oscillations and then a second transition back to a stable steady state which has not been observed in previously published models. On the basis of our results and following recent discussions about the role of delay-induced oscillations in gene transcription we establish the hypothesis that the period of the delay-induced cyclic changes should be characterized by an upper bound so that it cannot be greater than the period of fundamental biological cycles. We demonstrate our approach for two models. The first model describes Hes1 autorepression with equations for Hes1 mRNA production and Hes1 protein translation. The second model describes Hes1 repression by the protein complex Gro/TLE1/Hes1, where Gro/TLE1 is activated by Hes1 phosphorylation.

Keywords: gene expression with negative feedback, distributed time delay, limit cycle oscillations

---

\*Corresponding author. Tel: +49 381 498 7575, Fax: +49 381 7572

## Introduction

The three proteins Hes1, p53, and NF- $\kappa$ B are transcriptionally regulated by short negative feedback loops and actual experiments have revealed that their genes show an oscillatory expression [1, 2, 3, 4, 5]. In the vertebrate segmentation clock several cycling genes are involved in an oscillatory mechanism driving somite segmentation [6]. Mathematical models have been established for the regulation of these proteins [1, 2, 3, 5, 7, 8, 9, 10, 11, 12] where the authors of [7, 8, 9, 10] have introduced a discrete time delay to describe the time lag between transcription factor binding and gene transcription. Analytical and numerical results have shown that these models, which display damped oscillations for small positive delay times, can pass a Hopf bifurcation at a critical delay time where the stable steady state becomes unstable and a stable limit cycle oscillator emerges [7, 8, 9, 10].

Naturally, the question arises what the role of such oscillations in gene transcription could be [13, 14, 15, 16]? Due to the fact that the oscillation period is proportional to the delay time it may be possible that oscillations encode information. Single cell experiments have shown that the dynamics of NF- $\kappa$ B dependent transcription correlates with the duration of p65 oscillations [5, 14]. In other single cell experiments p53 has been expressed in a series of discrete pulses in response to DNA damage and the average number of pulses over all cells increased with the damage [4].

We introduce in our work a new model for gene transcription networks with a negative feedback loop where the time lag between transcription factor binding and mRNA production is described, in line with the natural variability, by a distributed time delay. With an increasing mean delay time this model can show a Hopf bifurcation leading to a transition from a stable steady state to an unstable steady state surrounded by a stable limit cycle oscillator and then a reverse Hopf bifurcation leading to a transition from a stable limit cycle oscillator to a stable steady state. Such a property has not been observed in previously published mathematical models for gene transcription networks. Following recent discussions about information encoding in delay-induced oscillations our results could be interpreted that the period of the delay-induced cyclic changes cannot be greater than the period of fundamental biological oscillations, say the cell cycle or the circadian clock. Therefore for a large delay time a reverse Hopf bifurcation should lead back to a stable steady state. This is demonstrated in our model.

The outline of the paper is as follows. The first section introduces differential equations with discrete and distributed time delays. In our model the distributed time delay is defined by a kernel of the Gamma function. The following two sections validate the approach with two models from the literature. The first model describes Hes1 autorepression with equations for Hes1 mRNA production and Hes1 protein translation. The second model describes Hes1 repression by the protein complex Gro/TLE1/Hes1, where Gro/TLE1 is activated by Hes1 phosphorylation. Our analytical and numerical results are discussed in relation to experimental data. This

leads us to an investigation into thresholds for damped and sustained oscillations.

## Discrete and distributed time delays

An appropriate mathematical representation to describe a time lag between an action and a reaction are delay differential equations [17]. If a variable influences the present state of the system at a fixed time point in the past,  $t - \tau$ , where  $\tau$  is the delay time, then the time lag can be modelled as a discrete delay

$$\frac{dx}{dt} = F(x, x(t - \tau)) .$$

A more realistic description of time lag effects in biological systems is to assume that the past influences the present state over an interval of time. Natural variability is weighted by a probability density  $\varrho$ , leading to a distributed delay

$$\frac{dx}{dt} = F\left(x, \int_0^\infty x(t - \tau) \varrho(\tau) d\tau\right) . \quad (1)$$

Analyzing a discrete delay differential equation through a Taylor series expansion of  $x(t - \tau)$  leads to an infinite dimensional system of ordinary differential equations. Approximations by a finite number of ordinary differential equations have been studied in [18, 19, 20]. In case of a distributed delay, we discuss below an example where a finite set of ordinary differential equations can exactly be derived. In either case, the increased dimension can lead to a stabilization or destabilization of the dynamics in feedback models.

Delay differential equations have been extensively applied to biological and engineering processes. This includes gene transcription [7, 8, 9, 10, 21, 22]; the nucleo-cytoplasmic translocation of proteins in eucaryotes [23, 24]; the hatching period and the incubation time in population models [25, 26]. In control theory the delay between the observation and the control of a variable has been considered [27, 28].

A frequently used model for distributed time delays in biological applications is to choose for the probability density  $\varrho$  in Eq. (1) the kernel of the Gamma function [18]

$$g_q^p(\tau) = \frac{q^p}{(p-1)!} \tau^{p-1} e^{-q\tau} , \quad (2)$$

which has a maximum at  $\tau = p/q$  and is zero at  $\tau = 0$  and for  $\tau \rightarrow \infty$ . The mean delay time is  $\bar{\tau} = (p+1)/q$ . This leads us to the following model

$$\frac{dx}{dt} = F\left(x, \int_0^\infty x(t - \tau) g_q^p(\tau) d\tau\right)$$

This model has the advantage that using the linear chain trick [18] we can transform the delay differential equations into a finite number of ordinary differential equations.

Authors that used this idea have found that distributed delay differential equations lead to a larger range of stability than discrete delay differential equations [26, 29, 30]. This is important in ecological models where the destabilization of the dynamics can lead to an extinction of species [26] or in physiological models where the disease is characterized by a stability change of a variable [29].

## Hes1 autorepression (Model I)

A mathematical model for Hes1 protein autorepression with a discrete time delay has been introduced in [7, 8, 9, 10]. The discrete time delay describes the time lag between Hes1 protein binding to the regulatory DNA and the production of Hes1 mRNA. For a critical delay time this model passes a Hopf bifurcation where the stable steady state is left and the system moves to a stable limit cycle [7, 8, 9, 10]. We here modify this model by replacing in Eqs. (3.1) and (3.2) of Ref. [10] the discrete time delay by a distributed time delay with Gamma kernel of Eq. (2), leading to

$$\begin{aligned}\frac{d}{dt}mRNA &= \frac{b \cdot k^h}{k^h + (\int_0^\infty Hes1(t-\tau) \cdot g_q^p(\tau) d\tau)^h} - a \cdot mRNA \\ \frac{d}{dt}Hes1 &= b \cdot mRNA - a \cdot Hes1.\end{aligned}\tag{3}$$

The first equation describes the temporal change of the Hes1 mRNA concentration, which depends on the autorepression by the Hes1 protein. The second equation describes the translation of the mRNA. We have implemented the distributed delay such that the averaging is performed over the transcription factor concentration reflecting the varying binding to their sites and the dissociation. In the linear case the smaller translation delay can be shifted into the transcription term without changing the dynamics [7]. Without loss of generality, we simplify Eqs. (3.1) and (3.2) of Ref. [10] by choosing the same rate constants for transcription and translation and also the same rate constant for degradations (cf. Table 1). We have chosen the parameter for the degradation rates ten-fold higher than in [10] so that the delay times which induce limit cycle oscillations are in the range of the temporal duration of gene transcription (10–40 min).

The first step in analyzing the properties of differential equations is to look for steady states and to study their stability. For  $k^h = (b/a)^h \cdot a/(b-a)$  the steady state of Eqs. (3) is  $mRNA^* = 1$  and  $Hes1^* = b/a$  which is stable for the case without delay [10]. Linear stability analysis of Eqs. (3) at steady state leads to the following eigenvalue equation

$$(\lambda + a)^2 + \frac{a^2 h}{b} (b - a) \int_0^\infty g_q^p(\tau) \cdot e^{-\lambda \tau} d\tau = 0.$$

The integral can be analytically solved, resulting in

$$(\lambda + a)^2 + \frac{a^2 h}{b}(b - a) \frac{q^p}{(\lambda + q)^p} = 0.$$

The eigenvalue equation is independent of how the averaging of the distributed time delay in Eqs. (3) is performed. The eigenvalue equation is the same regardless whether  $h$  is outside the integral as in Eqs. (3) or whether  $h$  is an exponent of  $Hes1(t - \tau)$ . The eigenvalue equation is also the same if we average over the transcription rate, i. e. ,

$$\int_0^\infty \frac{b \cdot k^h}{k^h + Hes1(t - \tau)^h} \cdot g_q^p(\tau) d\tau.$$

But it is different to the eigenvalue equation for the related model with a discrete time delay, Eq. (A13) in [10]. Thus considering natural variability in a delay differential equation model for Hes-protein autorepression can lead to different steady state dynamics, but the steady state dynamics is independent of the source of natural variability.

The next step is to analyze how the delay time influences the stability of the steady state by identifying critical mean delay times  $\bar{\tau} = (p + 1)/q$ , which form Hopf bifurcation points. First we apply the graphical method from Ref. [18] to get an immediate overview of putative Hopf bifurcations. We transform the eigenvalue equation with  $\lambda = \sigma + i\omega$  and  $\sigma = 0$  to

$$-\frac{b(i\omega + a)^2}{a^2 h(b - a)} = \frac{q^p}{(i\omega + q)^p} \quad (4)$$

Now the delay is separated into the delay curve on the right-hand-side (r.h.s.) of Eq. (4) and the ratio curve on the left-hand-side (l.h.s.). Both curves are plotted as a function of  $\omega$  in the complex plane in Fig. 1, together with the unit circle as the discrete delay curve. The shape of the delay curve does not depend on the scaling factor  $q$ . Intersections between a delay curve and a ratio curve are putative Hopf bifurcations. For several parameter pairs  $(p, h)$  two intersections occur indicating putative steady state – limit cycle – steady state transitions. For low values of  $p$  the system remains stable for low  $h$  or can pass through a steady state – limit cycle – steady state transition for higher  $h$ . For intermediate values of  $p$  three scenarios are possible: stable steady state for low  $h$ , steady state – limit cycle – steady state transitions for intermediate  $h$  and steady state – limit cycle transition for high  $h$ . For  $p \rightarrow \infty$  the delay curve converges to the discrete delay curve.

For  $p = 1$  and  $p = 2$ , Eq. (4) can be analytically solved for  $q$

$$q_{\pm} = a \left( c_p - 1 \pm \sqrt{(c_p - 1)^2 - 1} \right) \quad (5)$$

with

$$c_{p=1} = \frac{h}{4b}(b - a) \quad \text{and} \quad c_{p=2} = \frac{h}{2b}(b - a).$$

The critical mean delay times  $\bar{\tau}_{min}$  and  $\bar{\tau}_{max}$  for stability changes can be calculated from  $q_{\pm}$

$$\bar{\tau}_{min} = \frac{p+1}{q_+} \quad \text{and} \quad \bar{\tau}_{max} = \frac{p+1}{q_-}.$$

The parameter  $q$  in Eqs. (3) is chosen as the bifurcation parameter related to  $\bar{\tau}$ . The results for  $\bar{\tau}_{min}$  and  $\bar{\tau}_{max}$  are summarized in Table 1. This is compared to the results for the discrete delay according to Eq. (3.4) of [10]. The delay times of the two putative Hopf bifurcation points  $\bar{\tau}_{min}$  and  $\bar{\tau}_{max}$  are in the range of the duration of gene transcription. In addition, the results for  $a = 0.03$  (parameter value in [7, 10]) are shown in Table 2. For  $a = 0.03$  only the delay time of the first Hopf bifurcation point  $\bar{\tau}_{min}$  is in the range of the duration of gene transcription.

Comparing the distributed delay with the discrete delay shows that the distributed delay destabilizes at a higher critical mean delay time than the discrete delay. This is in agreement with the results in Refs. [26, 29, 30], where the authors have found that the distributed delay leads to a larger range of stability than with a discrete delay.

The following last step in our analysis is to check whether  $\sigma$  changes its sign at the critical values  $\bar{\tau}_{min}$  and  $\bar{\tau}_{max}$ . For most cases this is difficult or impossible to calculate analytically, which is why we used numerical simulations to check whether the two predicted Hopf bifurcations are passed. We transform Eqs. (3) with  $p = 2$  using the linear chain trick [18] to obtain

$$\begin{aligned} \frac{d}{dt}x_0 &= q \cdot (Hes1 - x_0) \\ \frac{d}{dt}x_1 &= q \cdot (x_0 - x_1) \\ \frac{d}{dt}mRNA &= \frac{b \cdot k^h}{k^h + x_1^h} - a \cdot mRNA \\ \frac{d}{dt}Hes1 &= b \cdot mRNA - a \cdot Hes1. \end{aligned} \tag{6}$$

Equations (6) represent a monotone cyclic feedback system. Several authors have focused on the existence of periodic solutions in such kind of equations [31, 32, 33, 34]. According to the Poincaré–Bendixson theorem for monotone cyclic feedback systems a stable solution of Eqs. (6) is either a stable steady state or a stable limit cycle oscillator [34]. Results from numerical simulations of Eqs. (6) with  $h = 6$  are presented in Fig. 2. The time course of the mRNA and Hes1 protein concentrations for delay times below and above the critical mean delay times show that the bifurcation at  $\bar{\tau}_{min}$  leads to a transition from a stable steady state to an unstable steady state. The latter is surrounded by a stable limit cycle oscillator. The reverse bifurcation at  $\bar{\tau}_{max}$  leads back to a stable steady state. Table 3 shows the frequency and the amplitude of the limit cycle oscillations as a function of the mean delay time. The frequency is inverse proportional to the delay time while the

amplitude has a maximum between the bifurcation points. Information can only be encoded in the frequency of the oscillations.

It follows that our model of Hes1 autorepression with a distributed delay has a maximal delay time for delay-induced limit cycle oscillations. This result is different to the discrete delay models [7, 8, 9, 10] which either show a steady state – limit cycle transition or no bifurcation. This can straightforwardly be shown for a generalized eigenvalue equation for these models, which reads  $(A - \lambda) \cdot (B - \lambda) - C \cdot e^{-\lambda\tau} = 0$ . The solution for purely imaginary eigenvalues  $\lambda = i\omega$  is  $w^2 = -(A^2 + B^2)/2 \pm \sqrt{((A^2 + B^2)^2/4 - A^2B^2 + C^2)}$  and  $\tau = 1/\omega \cdot \arccos((AB - \omega^2)/C)$ . Multiple solutions for  $\tau$  due to the periodicity of the angular function do not change stability [18]. Thus these two-dimensional negative feedback models for gene transcription with discrete time delay either show no Hopf bifurcation or they can show only one Hopf bifurcation but they can never show a Hopf bifurcation and a reverse Hopf bifurcation with increasing delay time. In contrast, a damped harmonic oscillator as an example from physics modelled with a discrete time delay can also show alternating stability and instability with increasing delay time [18].

The steady state properties of our model are independent on the way the averaging is performed in the distributed time delay. But they can depend on the kernel of the delay distribution. An alternative approach for a distributed time delay has been studied in [7]. The averaging is performed over the transcription rate but with a uniform kernel of the distribution on a finite support. In contrast to our results the results in [7] are indistinguishable from the discrete delay case. From our point of view, the Gamma kernel is a more realistic description for the probability density of a distributed time delay, because it has a maximum and approaches zero for  $\tau \rightarrow 0$  and  $\tau \rightarrow \infty$ .

The infinite support of the delay distribution in our model does not lead to an interference of the delay induced oscillations with fundamental biological oscillations for a broad parameter range because with increasing delay time the kernel of the Gamma function exponentially converges to zero. We calculate a boundary *max* such that the contribution of the tail of the delay distribution can be neglected:

$$\left( \int_0^{max} Hes1(t - \tau) g_q^p(\tau) d\tau + \int_{max}^{\infty} Hes1(t - \tau) g_q^p(\tau) d\tau \right)^h.$$

We consider only the expression with the highest contribution of the tail in this sum. Assuming  $Hes1 = 10$  as an upper boundary for the protein concentration. Lower boundaries for the parameter *max* for which the inequality

$$h \cdot \left( \int_0^{max} Hes1(t - \tau) g_q^p(\tau) d\tau \right)^{h-1} \cdot \int_{max}^{\infty} Hes1(t - \tau) g_q^p(\tau) d\tau < 10^{-6}$$

holds are  $max = 176\text{min}$  for  $h = 6$ ,  $\bar{\tau} = 16\text{min}$  and  $max = 672\text{min}$  for  $h = 10$ ,  $\bar{\tau} = 48\text{min}$  (critical delay times of reverse Hopf bifurcations). They are smaller for example then a typical time interval between two cell divisions in mammals of 24 hours or the circadian clock period.

## Gro/TLE1 mediated repression of Hes1 (Model II)

To see whether other models with a negative feedback loop can show a steady state – limit cycle – steady state transition, we consider what is referred to as Model C in [10]. Here Hes1 repression is realized by the protein complex Gro/TLE1/Hes1, denoted  $GroH$ , where Gro/TLE1 is activated by Hes1 phosphorylation. We replace in Eqs. (4.1) and (4.2) of Ref. [10] the discrete delay by a distributed delay with the Gamma kernel

$$\begin{aligned}\frac{d}{dt}Hes1 &= \frac{b \cdot k^h}{k^h + (\int_0^\infty g_q^p(\tau) \cdot GroH(t-\tau)d\tau)^h} - a \cdot Hes1 \\ \frac{d}{dt}GroH &= \frac{b \cdot Hes1^h}{l^h + Hes1^h} - a \cdot GroH.\end{aligned}\tag{7}$$

For  $k^h = a/(b-a)$  and  $l^h = (b-a)/a$  the steady state is  $Hes1^* = 1$  and  $GroH^* = 1$ . Linear stability analysis leads to the following eigenvalue equation at the steady state

$$0 = (\lambda + a)^2 + \frac{a^2 h^2}{b^2} (b-a)^2 \frac{q^p}{(\lambda + q)^p}$$

Again we apply the graphical method described above to get an overview of putative Hopf bifurcations or reverse Hopf bifurcations. Transformation of the eigenvalue equation with  $\lambda = \sigma + i\omega$  and  $\sigma = 0$  leads to

$$-\frac{b^2(i\omega + a)^2}{a^2 h^2 (b-a)^2} = \frac{q^p}{(i\omega + q)^p}\tag{8}$$

The ratio curve (l.h.s.) and the delay curve (r.h.s.) of Eq. (8) are shown in Figure 3. Several parameter pairs  $(p, h)$  show two putative Hopf bifurcations indicating stable steady state – limit cycle – stable steady state transitions.

The critical parameter  $q$  can be analytically calculated from Eq. (8) for  $p = 1$  and  $p = 2$

$$q_{\pm} = a \left( c_p - 1 \pm \sqrt{(c_p - 1)^2 - 1} \right)\tag{9}$$

with

$$c_{p=1} = \frac{h^2}{4b^2} (b-a)^2 \quad \text{and} \quad c_{p=2} = \frac{h^2}{2b^2} (b-a)^2.$$

The results for the critical mean delay times  $\bar{\tau}_{min}$  and  $\bar{\tau}_{max}$  are summarized in Table 1, together with the result for the discrete delay (according to Eq. (4.4) in [10]). The delay times of the two putative Hopf bifurcation points  $\bar{\tau}_{min}$  and  $\bar{\tau}_{max}$  are for some  $(p, h)$  pairs close to the range of the duration of gene transcription. The results for  $a = 0.03$  are shown in Table 2. For  $a = 0.03$  only the delay time of the first Hopf bifurcation point  $\bar{\tau}_{min}$  is close to the range of the duration for gene transcription.

Comparing the results for the distributed delay with those for the discrete delay shows that the distributed delay destabilizes at a larger critical mean delay time



than the discrete delay. This is in agreement with the results for Model I. Comparing now the critical delay times of Model I and II shows that Model II destabilizes at a lower critical delay time  $\bar{\tau}_{min}$  and stabilizes at a higher critical delay time  $\bar{\tau}_{max}$  than Model I. This is related to the stronger curvature of the ratio curve of Model II, which comes from cooperative repression together with cooperative activation whereas in Model I only cooperative repression is included.

For numerical simulations, we use the linear chain trick to derive for  $p = 2$  the ordinary differential equations

$$\begin{aligned}\frac{d}{dt}x_0 &= q \cdot (GroH - x_0) \\ \frac{d}{dt}x_1 &= q \cdot (x_0 - x_1) \\ \frac{d}{dt}Hes1 &= \frac{b \cdot k^h}{k^h + x_1^h} - a \cdot Hes1 \\ \frac{d}{dt}GroH &= \frac{b \cdot Hes1^h}{l^h + Hes1^h} - a \cdot GroH,\end{aligned}\tag{10}$$

The simulations confirm the two Hopf bifurcations as shown in Figure 4. The bifurcation at  $\bar{\tau}_{min}$  leads to a transition from a stable steady state to an unstable steady state, surrounded by a stable limit cycle oscillator. The reverse bifurcation at  $\bar{\tau}_{max}$  leads to a transition back to a stable steady state.

## Comparison with experimental results

In signaling and damage repair a fast response is desirable, which suggests that the initial reaction period is most important. This means that both, sustained and damped oscillations, are relevant for information encoding. The authors of Ref. [4] have measured discrete pulses for protein concentrations with fixed amplitude and duration, which do not depend on the amount of the stimulus. The experimental results in Ref. [5] show only few periods of the oscillations, making it difficult to decide whether one deals with sustained or damped oscillations. The same may be said for the results in [2]. A further complication arises from the difference between single-cell measurements, compared to averaging measurements. From a modelling perspective, sustained oscillations that arise after passing a Hopf bifurcation point, have a clear delay time threshold for frequency encoding signal transduction.

We now discuss possible thresholds for frequency encoding in damped oscillations. The mathematical models of Eqs. (3) and (7) show damped oscillations for large ranges of parameters without passing a Hopf bifurcation at a critical delay time. For other parameter ranges they approach a constant steady state. If damped oscillations are indeed relevant then the question after a threshold arises. A threshold is important to filter out noise which is an inherent property of biological signaling pathways. For damped oscillations a threshold could be the amplitude, which is however more sensitive to noise than the frequency of oscillations.

An alternative threshold for damped oscillation could be the critical delay time at which for the first time at least two eigenvalues switch from real numbers to complex numbers; while the real parts of all eigenvalues remain negative. Such a threshold can be calculated analytically for a one-dimensional Hes1 protein autorepression model (Model III)

$$\frac{d}{dt}Hes1 = \frac{b \cdot k^h}{k^h + (\int_0^\infty g_q^p(\tau) \cdot Hes1(t - \tau) d\tau)^h} - a \cdot Hes1 \quad (11)$$

Linear stability analysis of Eq. (11) with  $p = 1$  leads to the following eigenvalue equation

$$0 = \lambda + a + c \cdot \frac{q}{(\lambda + q)} \quad \text{with} \quad c = \frac{ha(b - a)}{b}$$

resulting in

$$\lambda_{1/2} = -\frac{a + q}{2} \pm \sqrt{\left(\frac{(a + q)^2}{4} - a \cdot q - c \cdot q\right)}.$$

From the zeros of the term under the square root

$$q_{1/2} = a + 2 \cdot c \pm \sqrt{((a + 2 \cdot c)^2 - a^2)} \quad (12)$$

we calculate the mean delay times  $\bar{\tau} = (p + 1)/q$  for transitions between real and complex eigenvalues. For  $\bar{\tau}$  below and above the transition values numerical simulations of exactly derived ordinary differential equations from Eq. (11) show no qualitative difference in the dynamics of the Hes1 protein concentrations, as shown in Figure 5. On the other hand, numerical simulations of Model I with parameters  $h = 6$ ,  $p = 2$  and  $a = 0.4$ , display for intermediate delay times damped oscillations with higher natural frequency, while for no and large delay times the oscillations have a lower natural frequency, as shown in Figure 6. The eigenvalues related to these parameters are complex for all delay times  $\tau \geq 0$  but no Hopf bifurcation is passed. The results shown in Figures 5 and 6 lead us to the conclusion that the first switch of two eigenvalues from real numbers to complex numbers is not an appropriate threshold.

Based on the results shown in Figures 5 and 6 we suggest as a quantitative measure for information encoding in the frequency of damped oscillations the ratio of frequency and damping defined by

$$\zeta = \frac{\omega}{\gamma}.$$

The values for  $\omega$  and  $\gamma$  are obtained from curve fits for the data in Figures 5 and 6 using the following equation

$$y = \alpha \cdot e^{-\gamma t} \cdot \cos(\omega t + \varphi).$$

This is motivated by the concept of a damping ratio in control engineering [27]. The results for  $\zeta$  are summarized in Table 4. The highest values for  $\zeta$  have the curves in Figure 6 (b) and (c).

## Summary and conclusions

In the present paper we investigated mathematical models for gene transcription networks with negative feedback loops. We described the time lag between transcription factor binding and mRNA production by a distributed time delay compared to previously published models which use a discrete delay. We applied our approach to describe experimentally observed oscillations of the transcription factor Hes1.

We showed that a distributed time delay can lead to limit cycle oscillations for a finite range of mean delay times  $[\bar{\tau}_{min}, \bar{\tau}_{max}]$ . We believe this to be a more realistic property of gene transcription networks with negative feedback if information is encoded in delay-induced oscillations. More specifically, we note that any oscillation period should not exceed the period of fundamental cellular processes, e.g. the cell cycle. This is an implicit property of our model with a Hopf bifurcation and a reverse Hopf bifurcation leading to steady state – limit cycle – steady state transitions.

Due to the possibility that both, sustained and damped oscillations could have a role in signal transmission we discussed the encoding of information in the frequency of the oscillations. Towards this end we proposed a quantitative measure for damped oscillations.

For future experimental work we suggest a more detailed experimental study into the nature of oscillations in gene transcription, investigating the consequences of pathological mutations that lead to abnormal time lags between transcription factor binding and mRNA production.

## Acknowledgements

We thank Nicholas Monk and Volkmar Liebscher for helpful comments on the manuscript. K.R. acknowledges support by the ministry for education, science and culture of the state Mecklenburg-Vorpommern and the “European Regional Development Fund” (ERDF). O.W.’s contributions were supported by the European Community as part of the FP6 project COSBICS and by the German Federal Ministry for Education & Research (BMBF) as part of the NGFNII SMP Protein.

# References

- [1] R.L. Bar-Or et al., Generation of oscillations by the p53–Mdm2 feedback loop: A theoretical and experimental study, *Proceedings of the National Academy of Science (USA)* 97(21) (2000) 11250–11255.
- [2] H. Hirata et al., Oscillatory expression of the bHLH factor Hes1 regulated by a negative feedback loop, *Science* 298 (2002) 840–843.
- [3] A. Hoffmann et al., The I $\kappa$ B–NF- $\kappa$ B signaling module: Temporal control and selective gene activation, *Science* 298 (2002) 1241–1245.
- [4] G. Lahav et al., Dynamics of the p53–Mdm2 feedback loop in individual cells, *Nature Genetics* 36(2) (2004) 147–150.
- [5] D.E. Nelson et al., Oscillations in NF- $\kappa$ B signaling control the dynamics of gene expression, *Science* 306 (2004) 704–708.
- [6] F. Giudicelli, J. Lewis, The vertebrate segmentation clock, *Current Opinion in Genetics & Development* 14(4) (2004) 407–414.
- [7] N.A.M. Monk, Oscillatory expression of Hes1, p53, NF- $\kappa$ B driven by transcriptional time delays, *Current Biology* 13 (2003) 1409–1413.
- [8] J. Lewis, Autoinhibition with transcriptional delay: A simple mechanism for the zebrafish somitogenesis oscillator, *Current Biology* 13 (2003) 1398–1408.
- [9] M.H. Jensen, K. Sneppen, G. Tian, Sustained oscillations and time delays in gene expression of protein Hes1, *FEBS Letters* 541 (2003) 176–177.
- [10] S. Bernard, B. Čajavec, L. Pujo-Menjouet, M.C. Mackey, H. Herzel, Modeling transcriptional feedback loops: The role of Gro/TLE1 in Hes1 oscillations, *Philosophical Transactions of the Royal Society A*, in press, (2005).
- [11] A. Ciliberto, B. Novak, J.J. Tyson, Steady states and oscillations in the p53/Mdm2 network, *Cell Cycle* 4(3) (2005) 107–112.
- [12] S. Zeiser, J. Müller, V. Liebscher, Modelling the Hes1 oscillator during somitogenesis, Manuscript submitted for publication, 2005.
- [13] G. Lahav, The strength of indecisiveness: Oscillatory behavior for better cell fate determination, *Science’s stke* 264 (2004) pe55.
- [14] D.E. Nelson, V. Sée, G. Nelson, M.R.H. White, Oscillations in transcription factor dynamics: a new way to control gene expression, *Biochemical Society Transactions* 32(6) (2004) 1090–1092.

- [15] D. Barken et al., Comment on “Oscillations in NF- $\kappa$ B signaling control the dynamics of gene expression”, *Science* 308 (2005) 52a.
- [16] D.E. Nelson et al., Response to comment on “Oscillations in NF- $\kappa$ B signaling control the dynamics of gene expression”, *Science* 308 (2005) 52b.
- [17] J.K. Hale, S.M. Verduyn Lunel, Introduction to Functional Differential Equations, Springer New York 4th edition, 1993.
- [18] N. MacDonald, Biological delay systems: linear stability theory, Cambridge University Press, 1989.
- [19] O.V. Matvii, I.M. Cherevko, On approximation of systems with delay and their stability, *Nonlinear Oscillations* 7(2) (2004) 207–215.
- [20] W.T. Mocek, R. Rudnicki, E.O. Voit, Approximation of delays in biochemical systems, *Mathematical Biosciences* 198 (2005) 190–216.
- [21] P. Smolen, D.A. Baxter, J.H. Byrne, Frequency selectivity, multistability, and oscillations emerge from models of genetic regulatory systems, *American Journal of Physiology - Cell Physiology* 274 (1998) 531–542.
- [22] P. Smolen, D.A. Baxter, J.H. Byrne, Effect of macromolecular transport and stochastic fluctuations on dynamics of genetic regulatory systems, *American Journal of Physiology - Cell Physiology* 277 (1999) 777–790.
- [23] I. Swameye, T.G. Müller, J. Timmer, O. Sandra, U. Klingmüller, Identification of nucleocytoplasmic cycling as a remote sensor in cellular signaling by data-based modeling, *Proceedings of the National Academy of Science (USA)* 100(3) (2003) 1028–1033.
- [24] S. Nikolov, V. Kotev, V. Petrov, An alternative approach for investigating a time delay model of the Jak–Stat signaling pathway, Manuscript submitted for publication, 2005.
- [25] R. May, Stability and complexity in model ecosystems, Princeton University Press, 2001.
- [26] C.W. Eurich, A. Thiel, L. Fahse, Distributed delays stabilize ecological feedback systems, *Physical Review Letters* 94(15) (2005) 158104–1–158104–4.
- [27] G.F. Franklin, J. David Powell, A. Emami-Naeini, Feedback Control of Dynamic Systems, Prentice Hall New Jersey 4th edition 2002.
- [28] W. Just, H. Benner, E. Schöll, Advances in Solid State Physics, volume 43, B. Kramer (Ed.), Springer, Berlin, 2003, pp. 589–603.

- [29] S. Bernard, J. Belair, M.C. Mackey, Sufficient conditions for stability of linear differential equations with distributed delay, *Discrete and Continuous Dynamical Systems B* 1(2) (2001) 233–256.
- [30] A. Thiel, H. Schwegler, C.W. Eurich, Complex dynamics is abolished in delayed recurrent systems with distributed feedback times, *Complexity* 8(4) (2003) 102–108.
- [31] B.C. Goodwin, Oscillatory behavior in enzymatic control processes, *Advance Enzyme Regulation* 3 (1965) 425–439.
- [32] J.J. Tyson, H.G. Othmer, The dynamics of feedback control circuits in biochemical pathways, *Progress in theoretical biology* 5 (1978) 1–62.
- [33] J.M. Mahaffy, Periodic solutions for certain protein synthesis models, *Journal of mathematical analysis and applications* 74 (1980) 72–105.
- [34] J. Mallet-Paret, H.L. Smith, The Poincaré-Bendixson theorem for monotone cyclic feedback systems, *Journal of Dynamics and Differential Equations* 2(4) (1990) 367–421.

Model	distributed		discrete
	$\bar{\tau}_{min}$	$\bar{\tau}_{max}$	
I:			
$h$ $p$			
6 2	6	16	2
8 2	3	33	0.2
10 2	2	48	0.1
II:			
$h$ $p$			
4 2	2	57	0.9
6 2	0.6	156	0.4
8 2	0.3	293	0.2
10 2	0.2	470	0.1
6 1	1	44	0.4
8 1	0.5	91	0.2

Table 1: Putative Hopf bifurcation points for distributed and discrete time delays. Delay times are given in minutes (min). For  $a = 0.3\text{min}^{-1}$  and  $b = 1\text{min}^{-1}$  analytical results from eigenvalue equation Eq. (5) for Model I and Eq. (9) for Model II. We have chosen the degradation rate  $a$  ten-fold higher than in Ref. [10] to ensure that the delay times are in the range of the time for gene transcription.

Model	distributed		discrete
	$\bar{\tau}_{min}$	$\bar{\tau}_{max}$	
I:			
$h$ $p$			
6   2	28	354	13
8   2	18	558	9
10   2	13	757	7
10   1	27	163	7
II:			
$h$ $p$			
4   2	8	1298	5
6   2	3	3184	2
8   2	2	5820	1
10   2	1	9208	1
4   1	12	356	5
6   1	4	991	2
8   1	2	1872	1
10   1	1	3002	1

Table 2: Putative Hopf bifurcation points, analytical results from eigenvalue equation Eq. (5) for Model I and Eq. (9) for Model II with  $a = 0.03\text{min}^{-1}$  and  $b = 1\text{min}^{-1}$ .

$\bar{\tau}$	frequency	amplitude
8	0.053	1.5
10	0.048	2.0
12	0.043	2.0
14	0.040	1.7

Table 3: Model I: Frequency and amplitude of limit cycle oscillations with increasing delay time for  $p = 2$ ,  $h = 6$  and  $a = 0.3\text{min}^{-1}$ .



	$\zeta = \omega/\gamma$		$\zeta = \omega/\gamma$	
$\bar{\tau}$	III:	$\bar{\tau}$	I: mRNA	I: protein
0.3	0	0	2	2
10	2	5	13	12
50	1	20	7	8
100	1	100	3	3

Table 4: Frequency damping ratio  $\zeta$  for the curves in Figures 5 (Model III) and 6 (Model I).

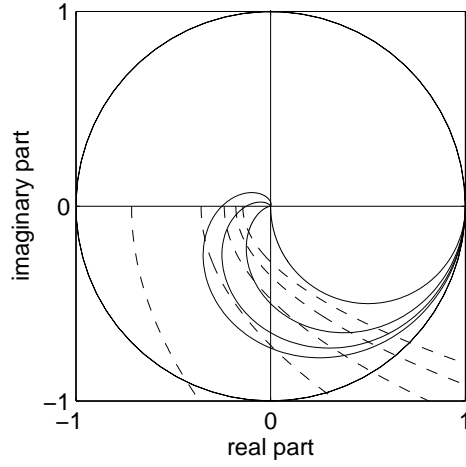


Figure 1: Model I: Intersections between the delay curves (solid lines) and the ratios curves (dashed lines). According to Eq. (4) intersections indicate putative Hopf bifurcations. The delay curves of the distributed time delay are shown for  $p = 1$  (in first quadrant only), 2, 3, 4 and the ratio curves are shown for  $h = 2$  (leftmost curve), 4, 6, 8, 10. In addition the unit circle as the discrete time delay curve is shown.

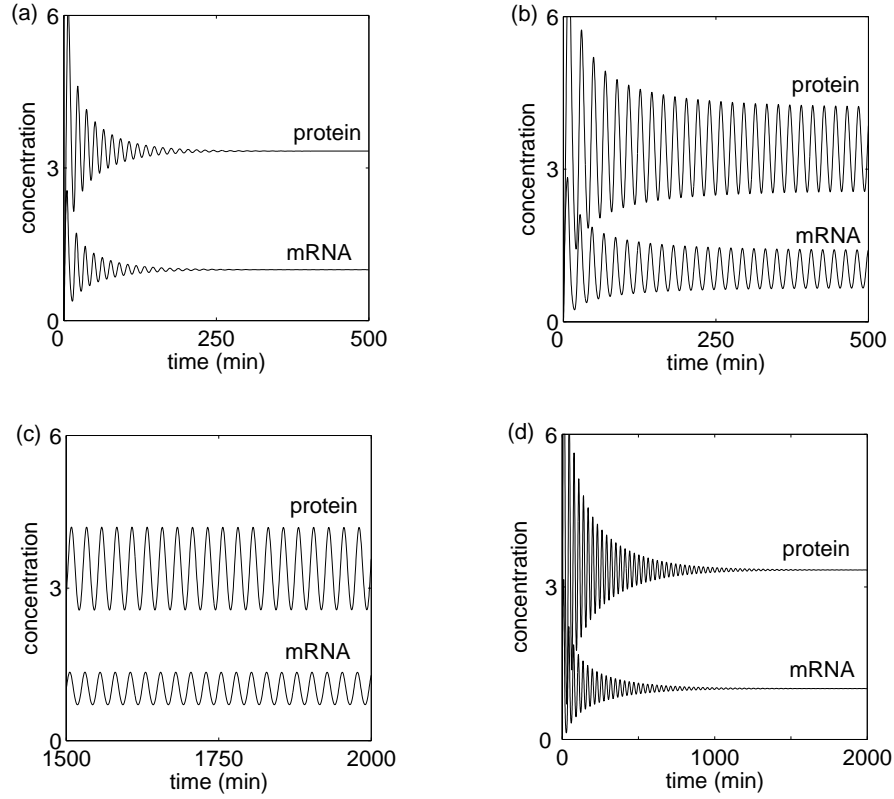


Figure 2: Model I: Numerical simulations of the exactly derived ordinary differential equations Eqs. (6) with  $p = 2$  and  $h = 6$ , showing a steady state – limit cycle – steady state transition by passing two Hopf bifurcation points with increasing mean delay time. (a)  $\bar{\tau} = 4$ , (b)  $\bar{\tau} = 8$ , (c)  $\bar{\tau} = 14$ , (d)  $\bar{\tau} = 20$ . Beyond the reverse Hopf bifurcation the damping of the oscillations increases with the delay time. For  $\bar{\tau} = 50$  the steady state is already reached at a time of 300min.

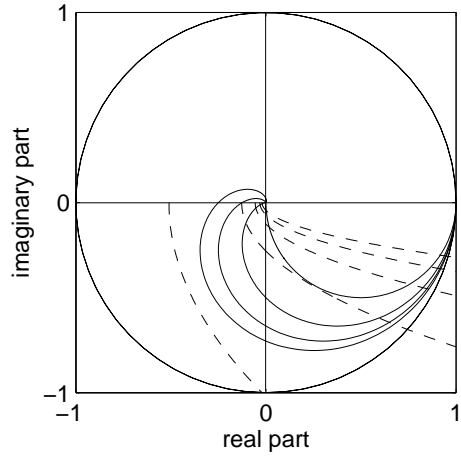


Figure 3: Model II: Intersections between the delay curves (solid line) and the ratio curves (dashed line). According to Eq. (8) intersections indicate putative Hopf bifurcations. The delay curves are shown for  $p = 1$  (first quadrant only), 2, 3, 4 and the ratio curves are shown for  $h = 2$  (most left curve), 4, 6, 8, 10.

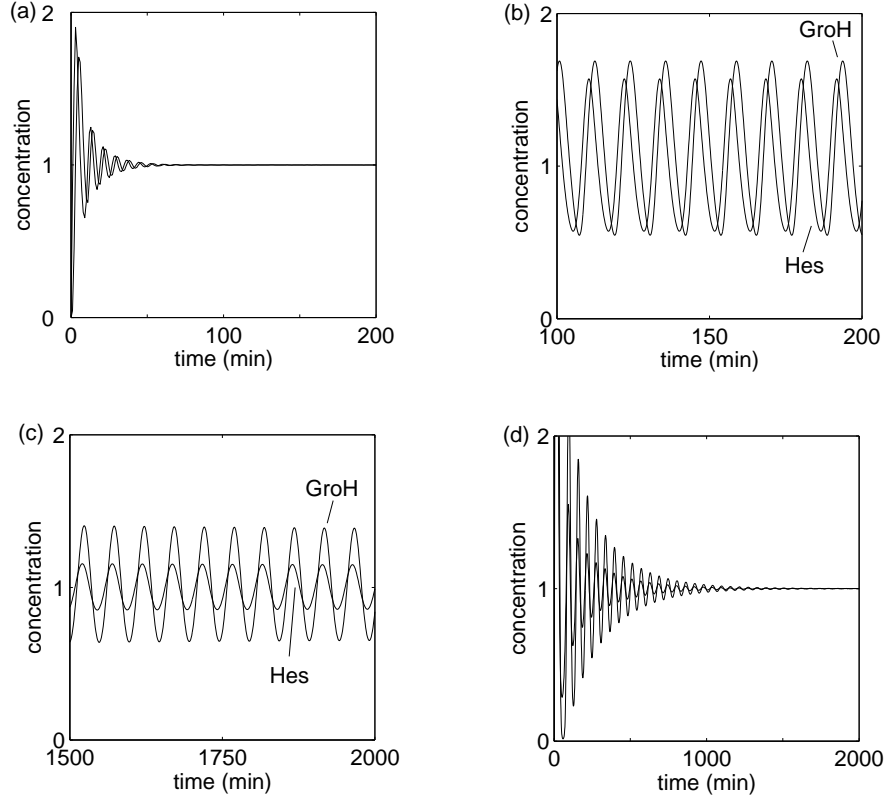


Figure 4: Model II: Numerical simulations of the exactly derived ordinary differential equations Eqs. (10) with  $p = 2$  and  $h = 4$ , showing a steady state – limit cycle – steady state transition by passing two Hopf bifurcation points with increasing mean delay time. (a)  $\bar{\tau} = 1$ , (b)  $\bar{\tau} = 3$ , (c)  $\bar{\tau} = 55$ , (d)  $\bar{\tau} = 70$ .

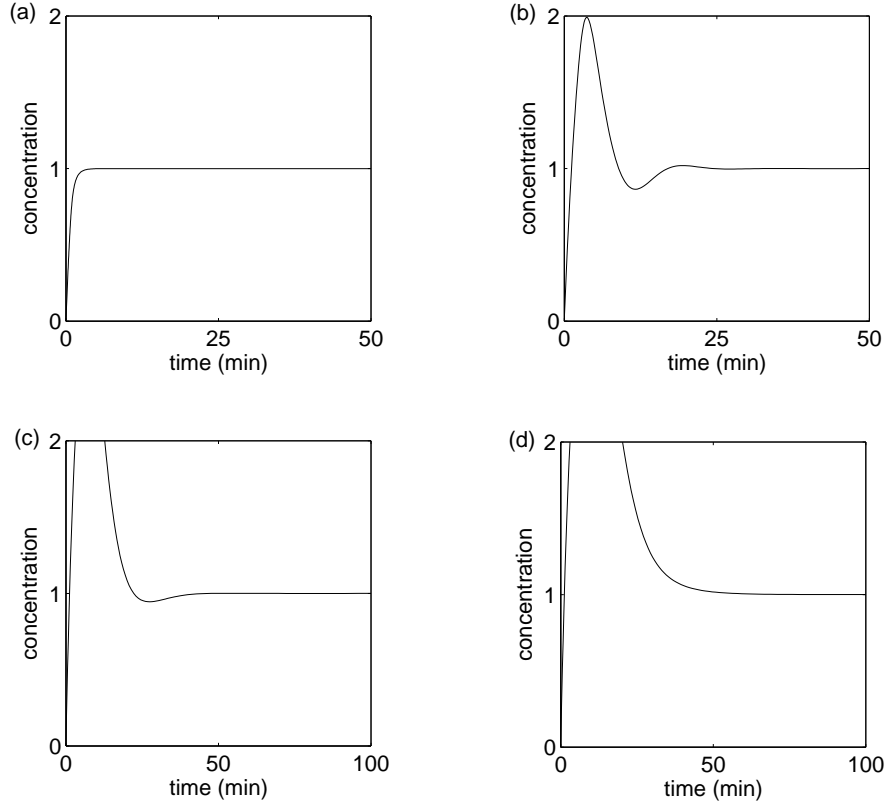


Figure 5: Model III: Numerical simulations of exactly derived ordinary differential equations from Eq. (11) with  $p = 1$  and  $h = 4$ , showing no pronounced damped oscillations. (a)  $\bar{\tau} = 0.3$  (b)  $\bar{\tau} = 10$  (c)  $\bar{\tau} = 50$  (d)  $\bar{\tau} = 100$ . Within the delay time interval  $[0.5, 87]$  the eigenvalues are complex according to Eq. (12).

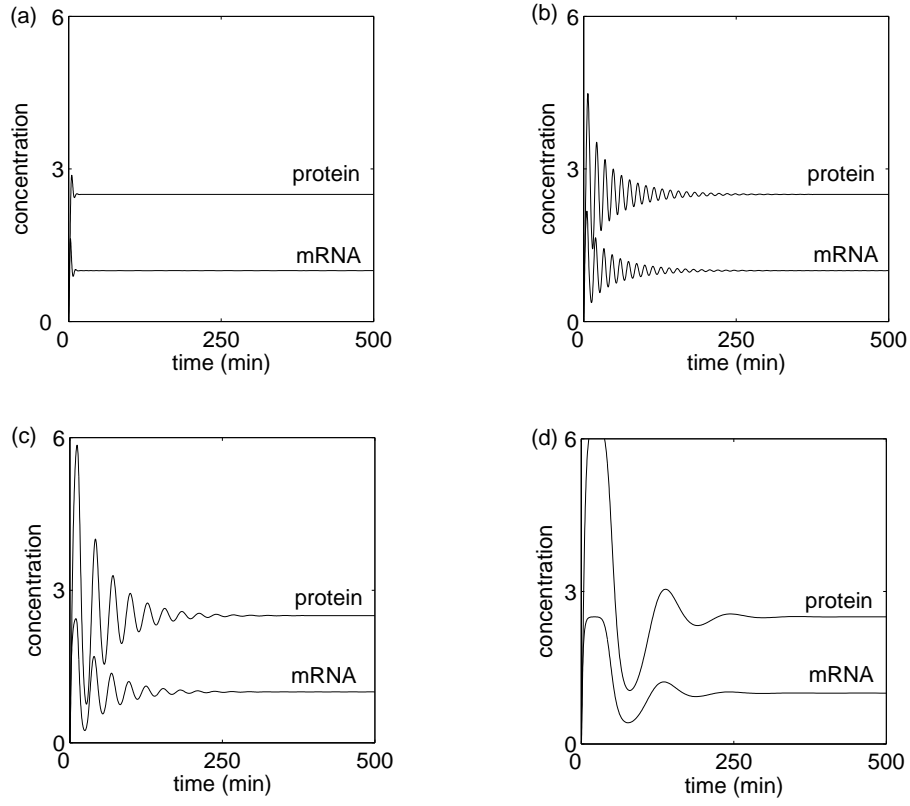


Figure 6: Model I: Numerical simulations of the exactly derived ordinary differential equations Eqs. (6) with  $p = 2$ ,  $h = 6$  and  $a = 0.4$ , showing for intermediate delay times pronounced damped oscillations without passing a Hopf bifurcation. (a)  $\bar{\tau} = 0$ , (b)  $\bar{\tau} = 5$ , (c)  $\bar{\tau} = 20$ , (d)  $\bar{\tau} = 100$ .